

## SUPPORTING INFORMATION

*Glycoconjugate journal*

### **The structure and role of lactone intermediates in linkage-specific sialic acid derivatization reactions**

**Tamas Pongracz<sup>1</sup>, Aswin Verhoeven<sup>1</sup>, Manfred Wuhrer<sup>1</sup>, Noortje de Haan<sup>1,\*†</sup>**

<sup>1</sup>Center for Proteomics and Metabolomics, Leiden University Medical Center, 2333ZA Leiden, The Netherlands

\*Corresponding author

[t.pongracz@lumc.nl](mailto:t.pongracz@lumc.nl); [a.verhoeven@lumc.nl](mailto:a.verhoeven@lumc.nl); [m.wuhrer@lumc.nl](mailto:m.wuhrer@lumc.nl); [ndehaan@sund.ku.dk](mailto:ndehaan@sund.ku.dk)

Correspondence: [ndehaan@sund.ku.dk](mailto:ndehaan@sund.ku.dk)

<sup>†</sup>Copenhagen Center for Glycomics, University of Copenhagen, 2200 Copenhagen, Denmark

## Table of contents:

**Supplementary Fig. 1.** MALDI-TOF-MS spectra (**a, b, d, e, g, h, j and k**) and bar graphs (**c, f, i and l**) showing the desired carboxyl group modification and the by-product introduced on the reducing end.

**Supplementary Fig. 2.** MALDI-TOF-MS spectra of sodium borohydride reduced  $\alpha$ 2,3- (**a-c**) and  $\alpha$ 2,6-sialyllactitol (**b-d**).

**Supplementary Fig. 3.** MALDI-FTICR-MS spectrum of (**a**) the isolation of the methyl esterified  $\alpha$ 2,3-sialyllactitol artifact at  $m/z$  672.238 introduced during the reduction protocol and (**b**) its MALDI-FT-ICR-MS/MS confirmation.

**Supplementary Fig. 4.** MALDI-TOF-MS spectra showing the modification induced on  $\alpha$ 2,3-sialyllactitol performed under native (**a-c**), direct (**d, e**) and control (**f-h**) EE conditions.

**Supplementary Fig. 5.** MALDI-TOF-MS spectra of the modification induced on  $\alpha$ 2,3-sialyllactitol performed under native (**a-c**), direct (**d, e**) and control (**f-h**) DMA conditions.

**Supplementary Fig. 6.** MALDI-TOF-MS spectra of the modification induced on  $\alpha$ 2,6-sialyllactitol performed under native (**a-c**), direct (**d, e**) and control (**f-h**) EE conditions.

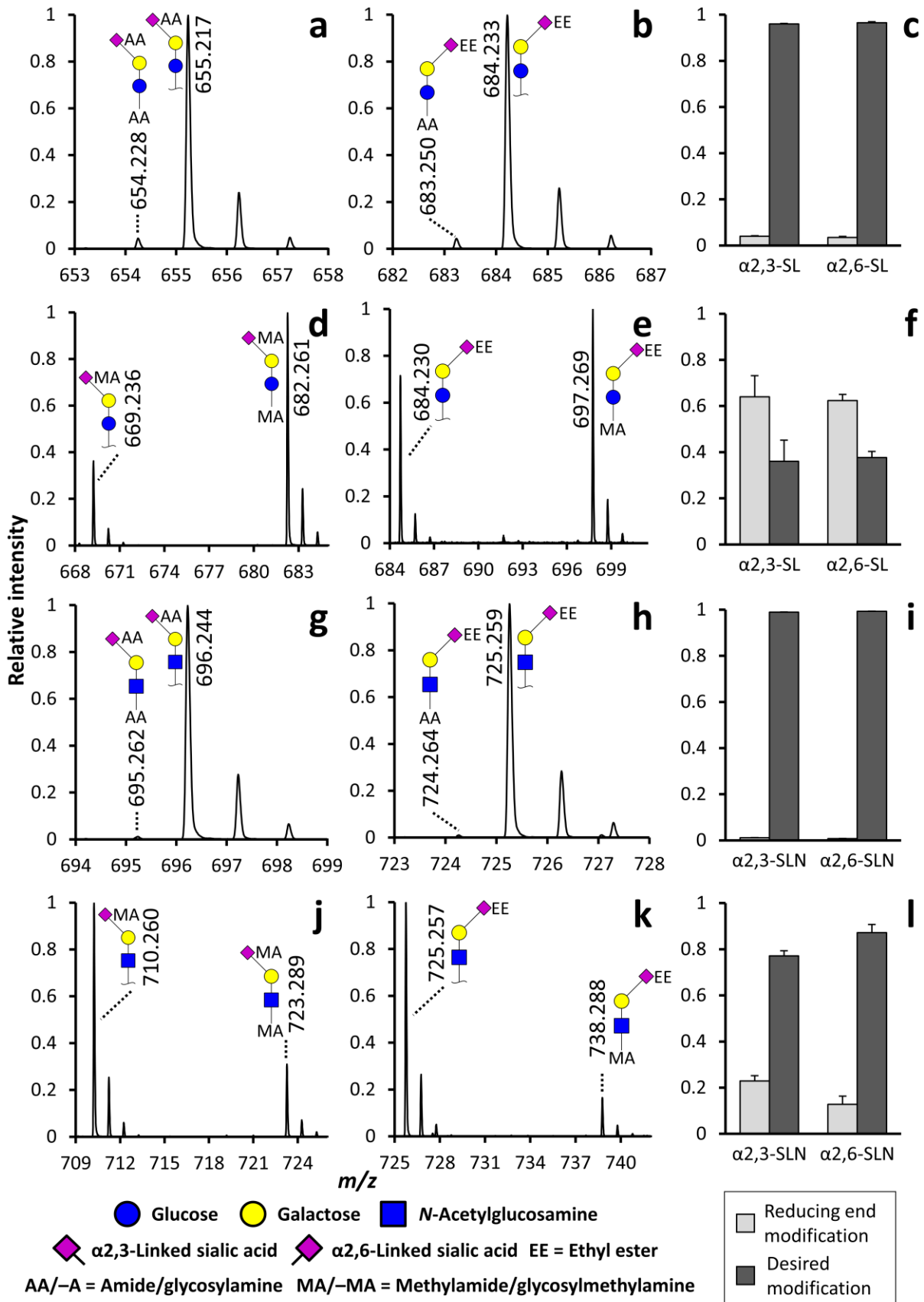
**Supplementary Fig. 7.** MALDI-TOF-MS spectra of the modification induced on  $\alpha$ 2,6-sialyllactitol performed under native (**a-c**), pre-basified (**d, e**) and control (**f-h**) DMA conditions.

**Supplementary Fig. 8.** Bar graphs illustrating the  $\text{NH}_3$  amidation and  $\text{MeNH}_2$  amidation step in EtOH (**a**) or DMSO (**b**) using an  $\alpha$ 2,6-sialyllactitol standard.

**Supplementary Fig. 9.** Representative MALDI-FTICR-MS spectra of complex type *N*-glycans deriving from rhEPO under the tested conditions (**a-e**).

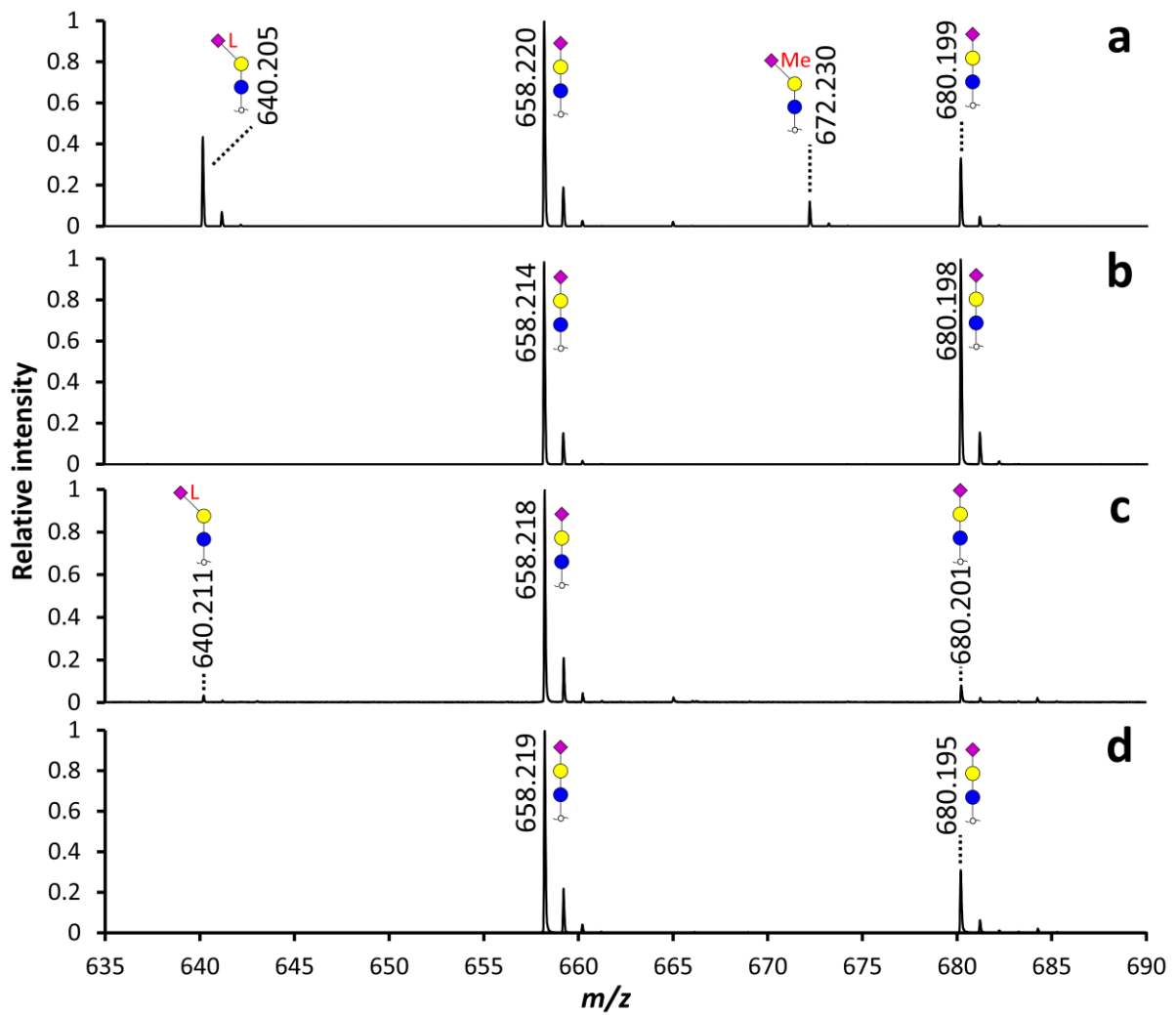
**Supplementary Fig. 10.** Representative MALDI-FTICR-MS spectra of complex type *N*-glycans deriving from IgG under the tested conditions (**a-e**).

**Supplementary Fig. 11.** Reaction products observed for  $\alpha$ 2,6-linked *N*-glycans from IgG under the tested conditions.

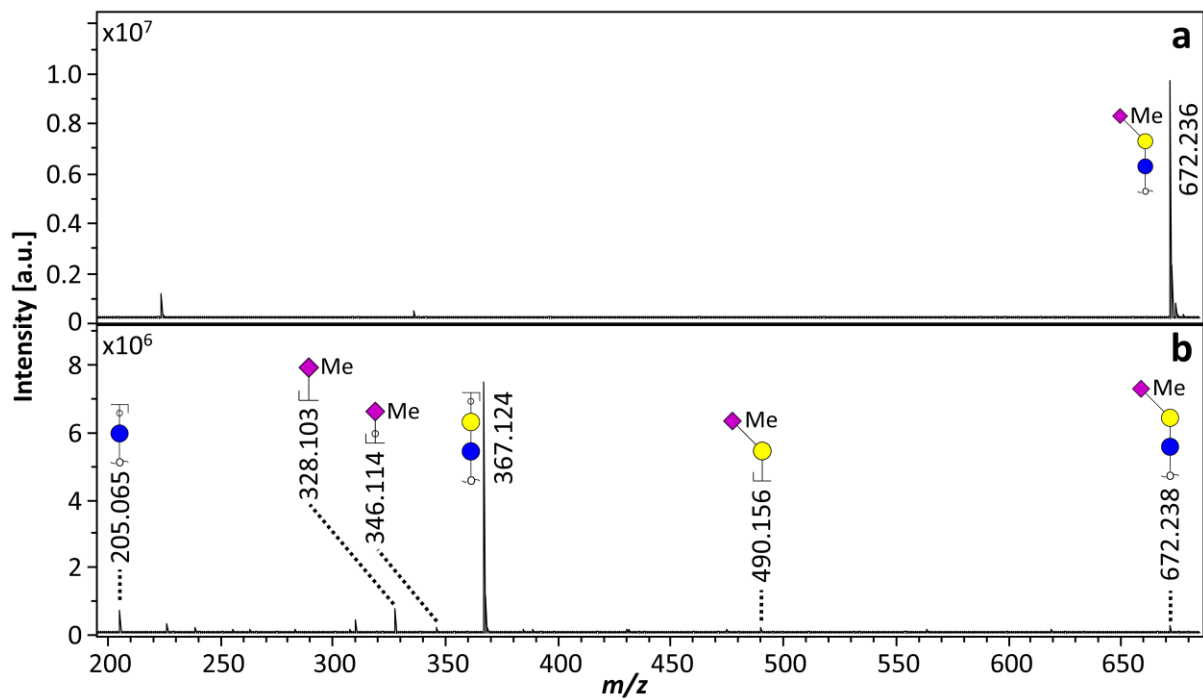


**Supplementary Fig. 1.** MALDI-TOF-MS spectra (a, b, d, e, g, h, j and k) and bar graphs (c, f, i and l) showing the desired carboxyl group modification and the by-product introduced on the reducing end. The glycosylamine introduced on the NH<sub>3</sub> amidated  $\alpha$ 2,3- (a) and ethyl esterified  $\alpha$ 2,6-sialyllactose (b)

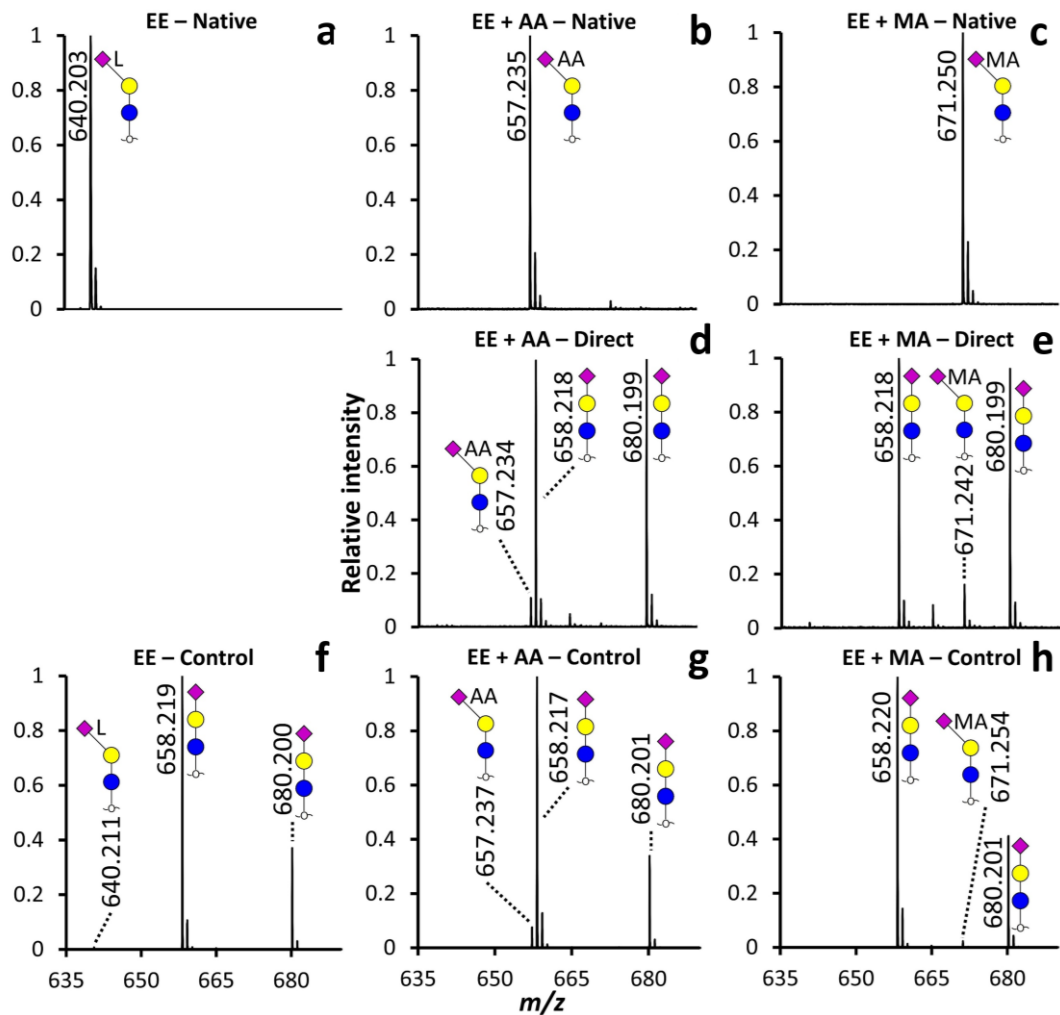
or  $\text{NH}_3$  amidated  $\alpha 2,3$ - (**g**) and ethyl esterified  $\alpha 2,6$ -sialylLacNAc (**h**) was observed at  $m/z$  -0.984 from the peak with the desired modification. The glycosylmethylamine introduced on the  $\text{MeNH}_2$  amidated  $\alpha 2,3$ - (**d**) and ethyl esterified  $\alpha 2,6$ -sialyllactose (**e**), or  $\text{MeNH}_2$   $\alpha 2,3$ - (**j**) and ethyl esterified  $\alpha 2,6$ -sialylLacNAc (**k**) was observed at  $m/z$  +13.032 from the peak with the expected modification. The  $\alpha 2,3$ -linkages are depicted with a left angle, with  $\text{NH}_3$  amidation indicated by AA and  $\text{MeNH}_2$  amidation by MA next to the sialic acid residue. The  $\alpha 2,6$ -linkages are depicted with a right angle, with ethyl esterification indicated by EE next to the sialic acid residue. Reducing end modifications are indicated as -AA (glycosylamine) and -MA (glycosylmethylamine). All species were detected as  $[\text{M}+\text{Na}]^+$ .



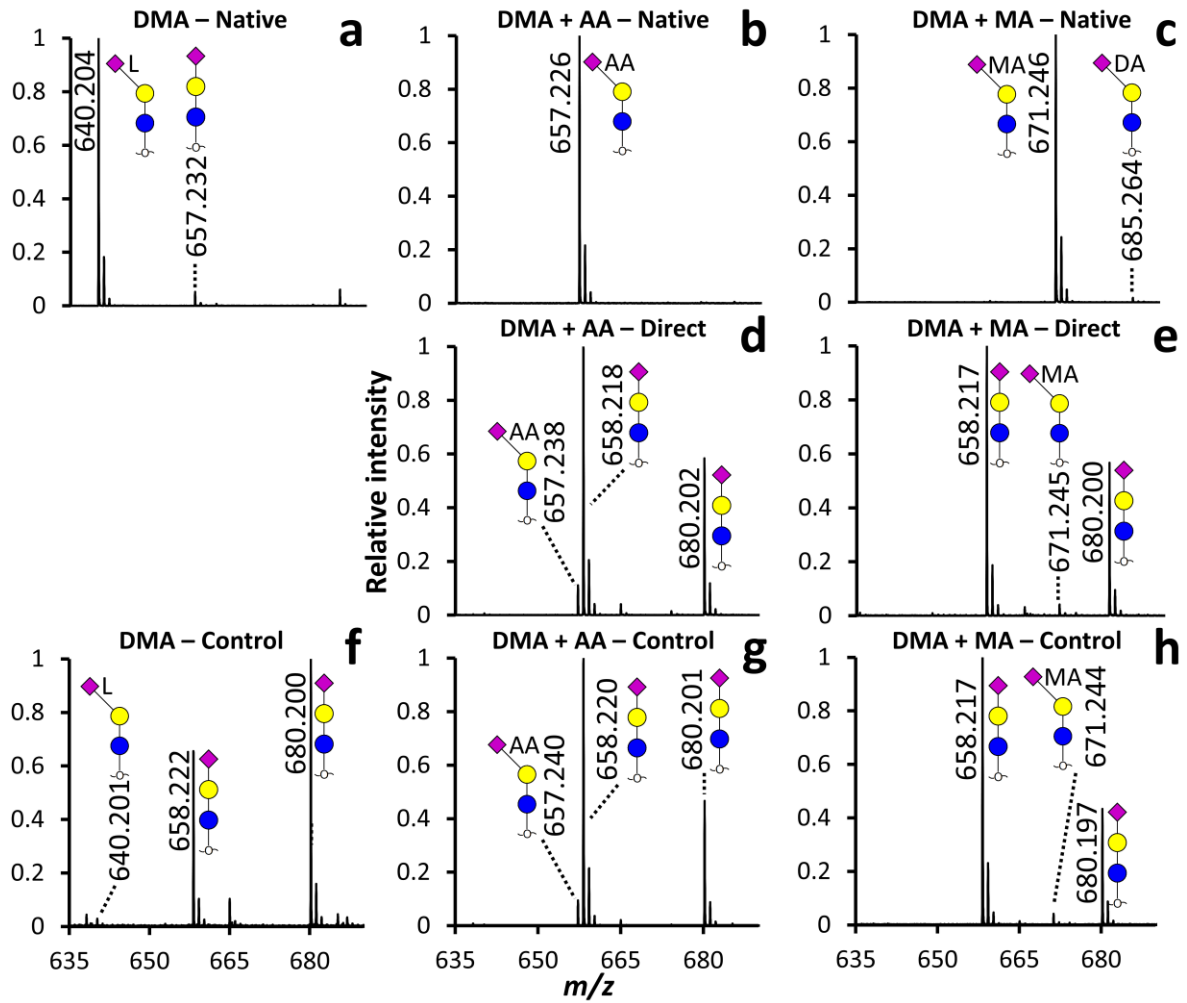
**Supplementary Fig. 2.** MALDI-TOF-MS spectra of sodium borohydride reduced  $\alpha$ 2,3- (**a-c**) and  $\alpha$ 2,6-sialyllactitol (**b-d**). Methanol (**a-b**) or isopropanol (**c-d**) was used for bead conditioning before cation-exchange clean-up and as co-evaporating agent during three consecutive borate removal steps in the SpeedVac concentrator. In case of derivatized sialic acids, an  $\alpha$ 2,3-linkage is depicted with a left angle, with undesired modifications indicated by L (lactonization), and Me (methyl esterification) in red next to the sialic acid residue. Non-derivatized sialic acids are depicted without an angle, and were detected as both  $[M+Na]^+$  and  $[M-H+2Na]^+$ .



**Supplementary Fig. 3.** MALDI-FTICR-MS spectrum of (a) the isolation of the methyl esterified  $\alpha$ 2,3-sialyllactitol artifact at  $m/z$  672.238 introduced during the reduction protocol and (b) its MALDI-FTICR-MS/MS confirmation.

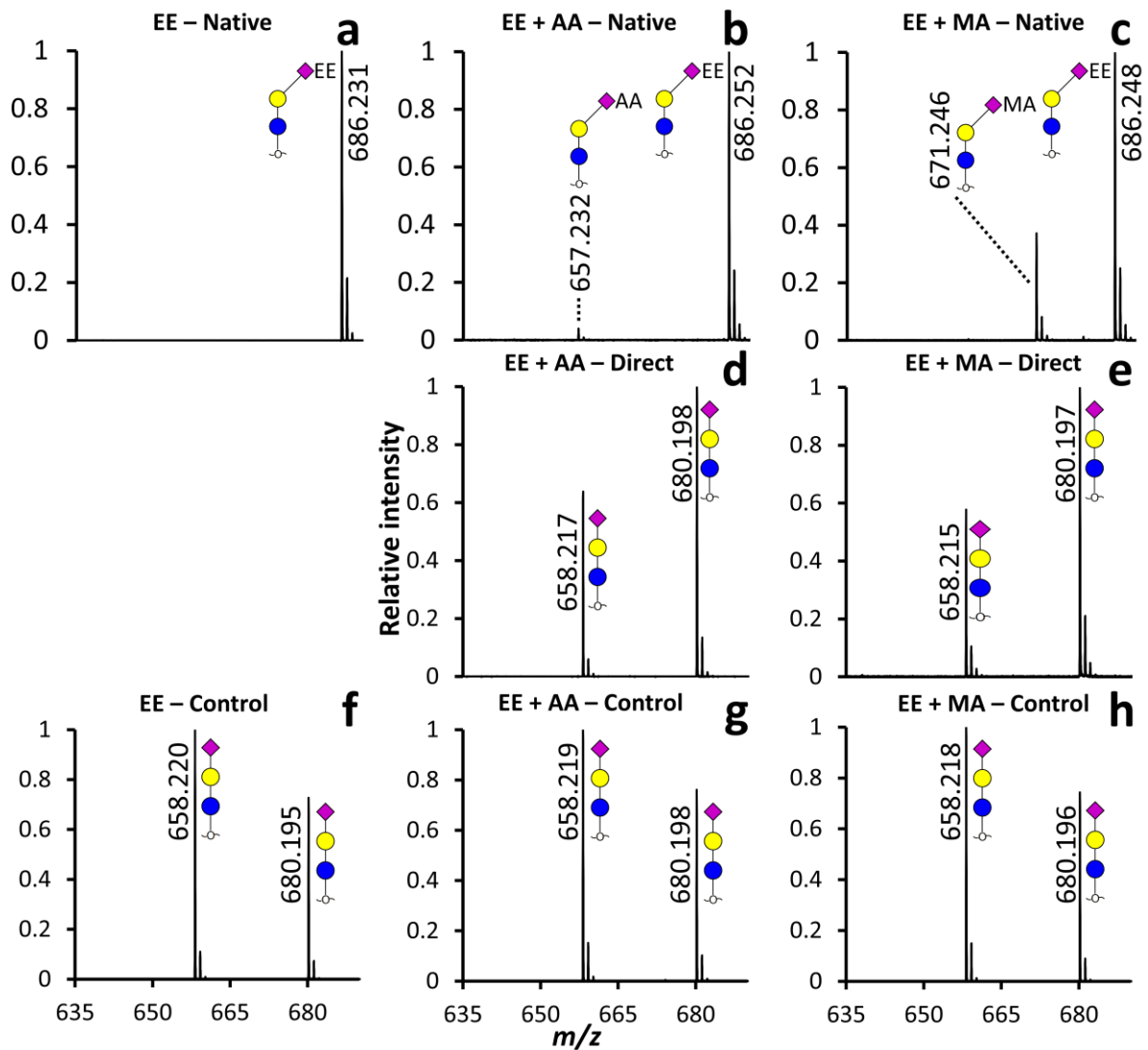


**Supplementary Fig. 4.** MALDI-TOF-MS spectra showing the modification induced on  $\alpha$ 2,3-sialyllactitol performed under native (a-c), direct (d, e) and control (f-h) EE conditions. In case of derivatized sialic acids, an  $\alpha$ 2,3-linkage is depicted with a left angle, with lactonization indicated by L,  $\text{NH}_3$  amidation by AA, and  $\text{MeNH}_2$  amidation by MA next to the sialic acid residue. Non-derivatized sialic acids are depicted without an angle, and were detected as both  $[\text{M}+\text{Na}]^+$  and  $[\text{M}-\text{H}+2\text{Na}]^+$ .

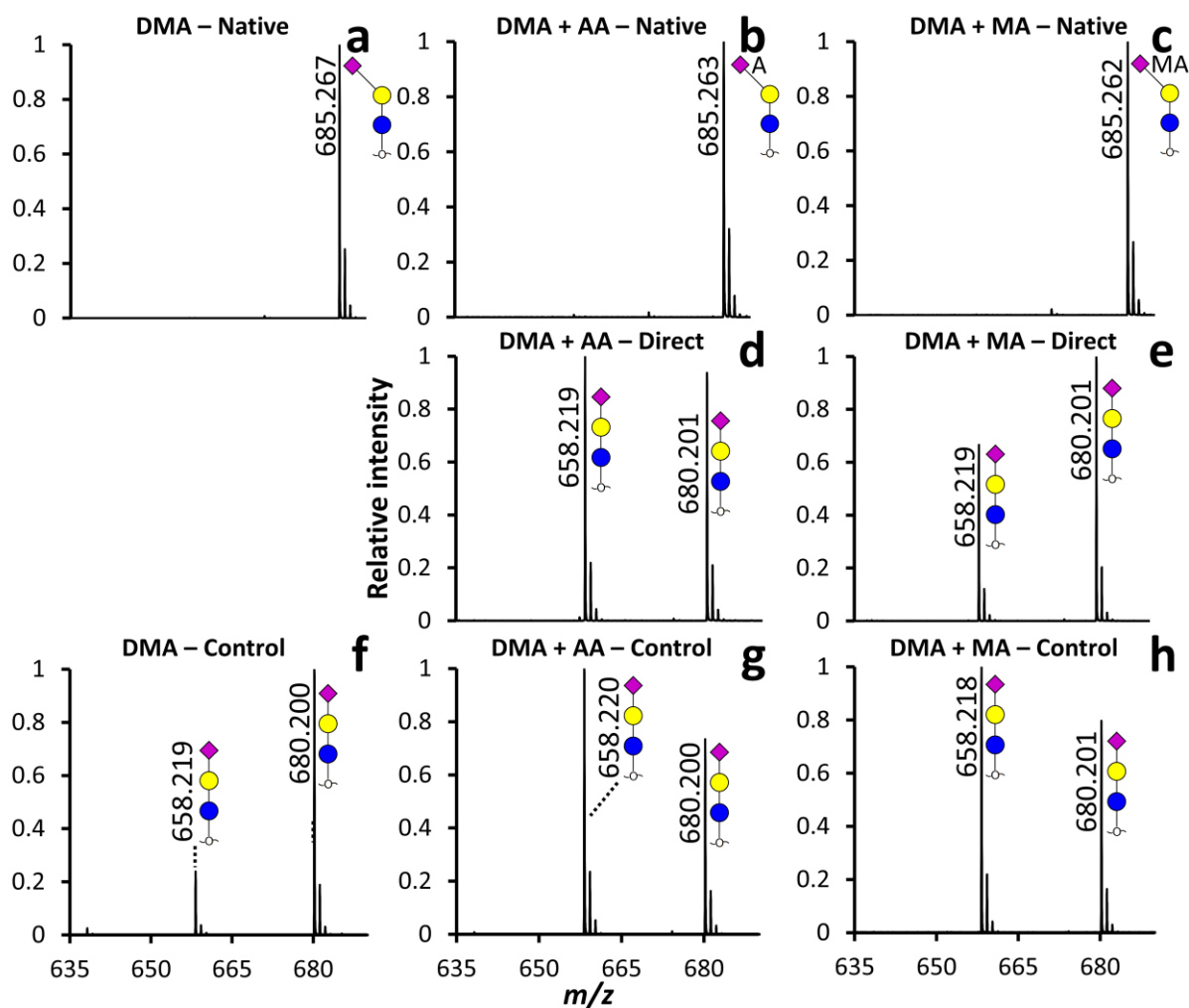


**Supplementary Fig. 5.** MALDI-TOF-MS spectra of the modification induced on  $\alpha$ 2,3-sialyllactitol performed under native (**a-c**), direct (**d, e**) and control (**f-h**) DMA conditions. In case of derivatized sialic acids, an  $\alpha$ 2,3-linkage is depicted with a left angle, with lactonization indicated by L,  $\text{NH}_3$  amidation by AA and  $\text{MeNH}_2$  amidation by MA next to the sialic acid residue. Non-derivatized sialic acids are depicted without an angle, and were detected as both  $[\text{M}+\text{Na}]^+$  and  $[\text{M}-\text{H}+2\text{Na}]^+$ .

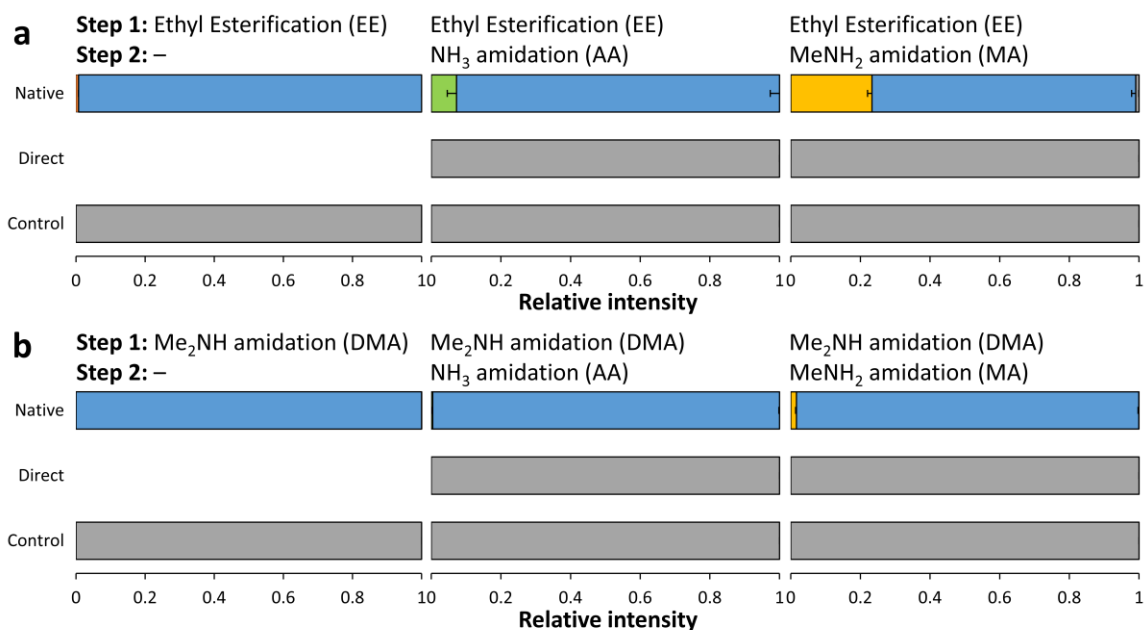




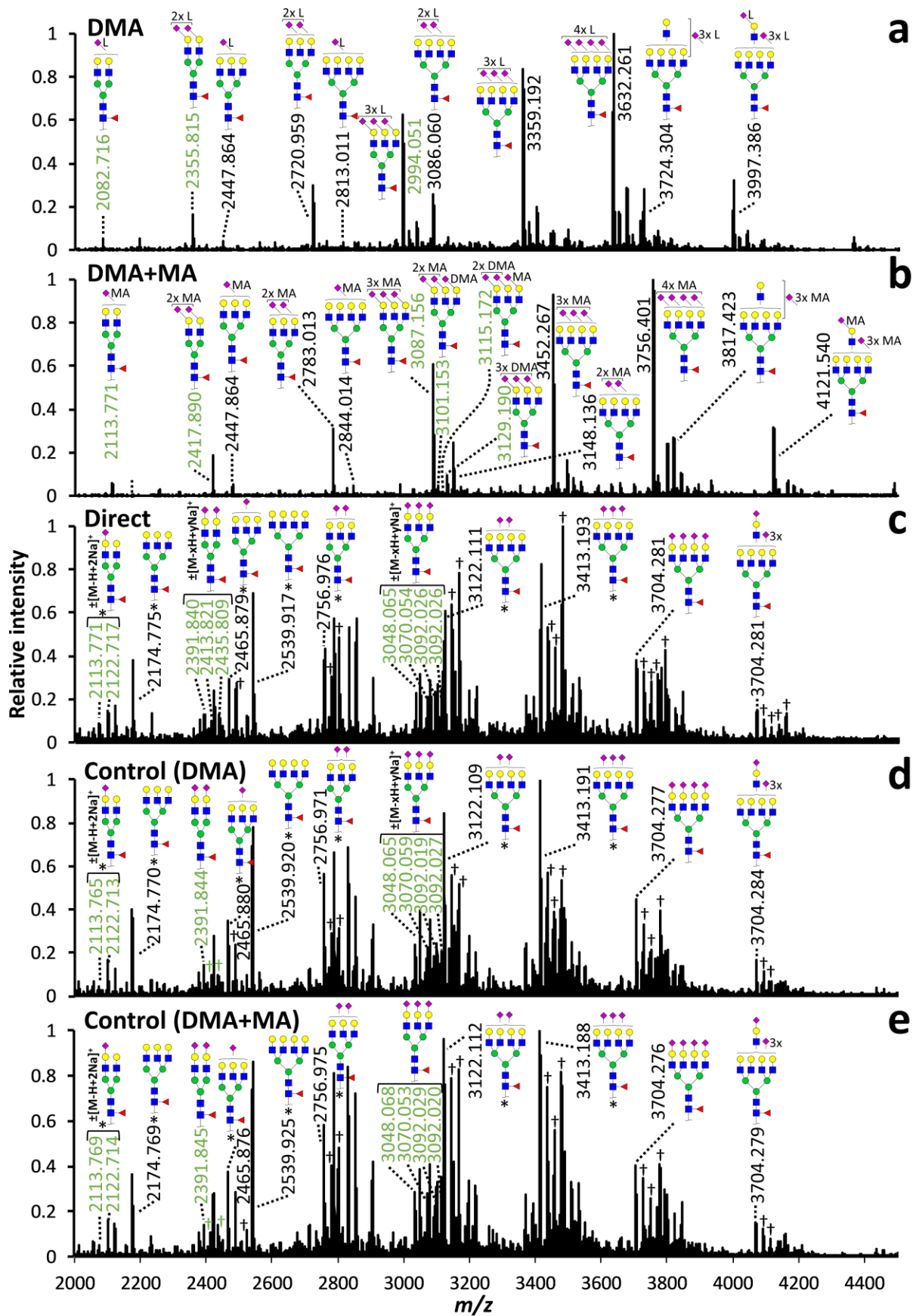
**Supplementary Fig. 6.** MALDI-TOF-MS spectra of the modification induced on  $\alpha$ 2,6-sialyllactitol performed under native (a-c), direct (d, e) and control (f-h) EE conditions. In case of derivatized sialic acids, an  $\alpha$ 2,6-linkage is depicted with a right angle, with  $\text{NH}_3$  amidation indicated by AA,  $\text{MeNH}_2$  amidation by MA and ethyl esterification by EE next to the sialic acid residue. Non-derivatized sialic acids are depicted without an angle. Non-derivatized sialic acids were detected as both  $[\text{M}+\text{Na}]^+$  and  $[\text{M}-\text{H}+2\text{Na}]^+$ .



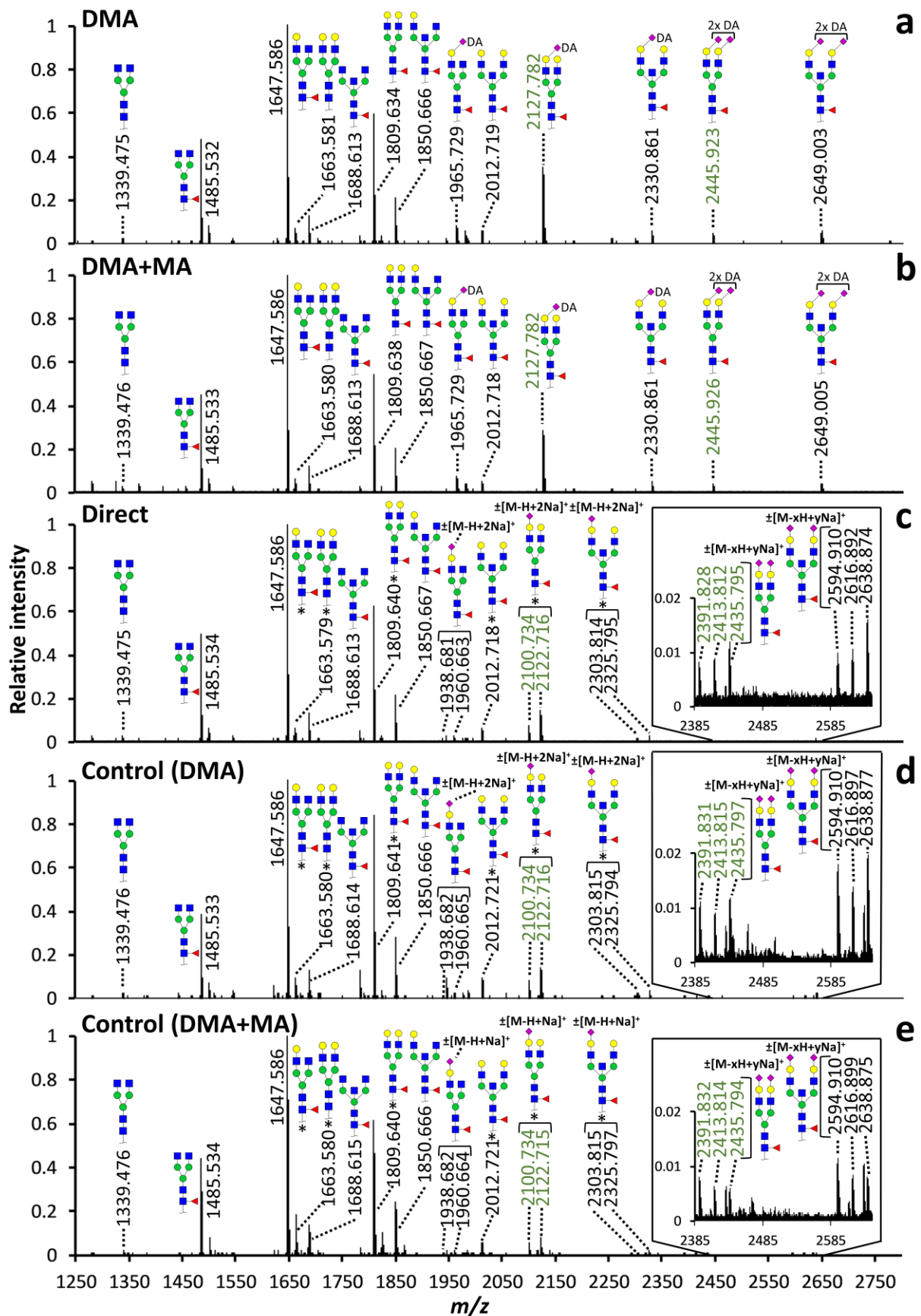
**Supplementary Fig. 7.** MALDI-TOF-MS spectra of the modification induced on  $\alpha$ 2,6-sialyllactitol performed under native (a-c), pre-basified (d, e) and control (f-h) DMA conditions. In case of derivatized sialic acids, an  $\alpha$ 2,6-linkage is depicted with a right angle, with  $\text{NH}_3$  amidation indicated by AA,  $\text{MeNH}_2$  amidation by MA and ethyl esterification by EE next to the sialic acid residue. Non-derivatized sialic acids are depicted without an angle, and were detected as both  $[\text{M}+\text{Na}]^+$  and  $[\text{M}-\text{H}+2\text{Na}]^+$ .



**Supplementary Fig. 8.** Bar graphs illustrating the NH<sub>3</sub> amidation and MeNH<sub>2</sub> amidation step in EtOH (a) or DMSO (b) using an  $\alpha$ 2,6-sialyllactitol standard. Native reaction conditions refer to the application of either EE or DMA reagent in the first step of the reaction and the addition of NH<sub>3</sub> or MeNH<sub>2</sub> in the second step. The direct conditions mimic the NH<sub>3</sub> amidation or MeNH<sub>2</sub> amidation step by the immediate addition of NH<sub>4</sub>OH or MeNH<sub>2</sub> in the first step. The control conditions refer to the use of control-reagents without EDC and HOBt following the two-step reaction. The average and SDs for triplicate measurements are shown as stacked bars and error bars, respectively. Total area normalization was performed on the indicated species following data curation (**Supplementary Table 6**). The pH of the conditions was evaluated in triplicate using narrow range pH indicator strips (**Supplementary Table 1**).

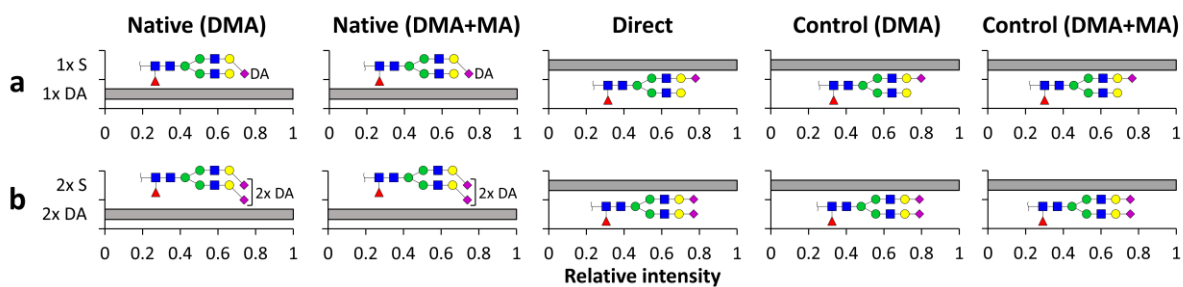


**Supplementary Fig. 9.** Representative MALDI-FTICR-MS spectra of complex type *N*-glycans deriving from rhEPO under the tested conditions (**a-e**). In case of derivatized sialic acids, an  $\alpha$ 2,3-linkage is depicted with a left angle, with lactonization indicated by L, MeNH<sub>2</sub> amidation by MA, and Me<sub>2</sub>NH amidation by DA next to the sialic acid residue. Non-derivatized sialic acids are depicted without an angle. The x indicator in the (mass definer) is a multiplier as 1, 2 or 3, while the y indicator in the (mass definer) is a multiplier as 2, 3 or 4. The *m/z* values highlighted in green indicate structures that have been selected for visualization in (**Fig. 5**). Glycans labelled with an asterisk (\*) denote potential in-source decay fragments. Peaks labelled with a cross (†) denote sialylated glycan signals that derive from neighboring peaks that underwent multiple carboxylic proton-to-sodium exchanges and are not depicted due to spatial constraints.



**Supplementary Fig. 10.** Representative MALDI-FTICR-MS spectra of complex type *N*-glycans deriving from IgG under the tested conditions (a-e). In case of derivatized sialic acids, an  $\alpha$ 2,6-linkage is depicted with a right angle, with Me<sub>2</sub>NH amidation indicated by DA next to the sialic acid residue.

The x indicator in the (mass definer) is a multiplier as 1 or 2, while the y indicator in the (mass definer) is a multiplier as 2 or 3. The  $m/z$  values highlighted in green indicate structures that have been selected for visualization in **(Supplementary Fig. 11)**. Insets **(c-e)** show the  $m/z$  range of 2385-2650. No indication for mis-conversion or under-modification has been observed **(a, b)**. Glycans labelled with an asterisk (\*) denote potential in-source decay fragments.



**Supplementary Fig. 11.** Reaction products observed for  $\alpha 2,6$ -linked *N*-glycans from IgG under the tested conditions. **(a)** H5N4F1S1 and **(b)** H5N4F1S2 are the gross glycan compositions evaluated. Abbreviations indicate H (hexose); N (*N*-acetylgalactosamine); F (fucose); S (*N*-acetylneuraminic acid). Symbols indicate the monosaccharide residues mannose (green circle), galactose (yellow circle) and *N*-acetylneuraminic acid (purple diamond). In case of derivatized sialic acids, an  $\alpha 2,6$ -linkage is depicted with a right angle, with  $\text{Me}_2\text{NH}$  amidation indicated by DA next to the sialic acid residue. Non-derivatized  $\alpha 2,6$ -sialic acids are depicted without an angle. The average and SDs for triplicate measurements are shown as bars and error bars, respectively. Total area normalization was performed on the indicated species following data curation (**Supplementary Table 7**).